Int. J. Res. Ind. Eng. Vol. 9, No. 1 (2020) 1–12

International Journal of Research in Industrial Engineering
www.riejournal.com

Factual Power Loss Reduction by Augmented Monkey Optimization Algorithm

L. Kanagasabai*

Department of EEE, Prasad V. Potluri Siddhartha Institute of Technology, Kanuru, Vijayawada.

A B S T R A C T

This paper presents Augmented Monkey Optimization Algorithm (AMOA) applied to solve optimal reactive power problem. Communal behaviour of monkeys has been utilized to model the algorithm. Normally, group monkeys assess the distance from the source to food for foraging behaviour. Local leader renews its most excellent location inside the group, when the food source is not rationalized then the group will start probing in different directions for the food sources. Two most important control parameters are Global Leader Limit (GLlimit) and Local Leader Limit (LLlimit) which give appropriate way to global and local leaders correspondingly. Levy flight has been intermingled in the algorithm to enhance the search ability. Proposed AMOA accelerates the exploitation ability that has been tested in standard IEEE 14, 30, 57,118,300 bus test systems. The simulation results show the projected algorithm reduced the real power loss comprehensively.

Keywords: Optimal reactive power, Transmission loss, Augmented monkey optimization algorithm.

Article history: *Received: 04 October 2019* *Revised: 12 January 2020* *Accepted: 17 February 2020*

1. Introduction

Reactive power problem plays a key role in secure and economic operations of power system. Optimal reactive power problem has been solved by variety of types of methods [1-6]. Nevertheless, numerous scientific difficulties are found while solving problem due to an assortment of constraints. Evolutionary techniques [7-16] are applied to solve the reactive power problem, but the main problem is the many algorithms get stuck in local optimal solution and fail to balance the exploration and exploitation during the search of global solution. In this paper, AMOA has been applied to solve the optimal reactive power problem. Communal behavior of monkeys has been utilized to model the algorithm. Normally, group monkeys assess the distance from the source to food for foraging behavior. Based on the distance from the foods source, the

* Corresponding author
E-mail address: gklenin@gmail.com
DOI: 10.22105/riej.2020.214459.1112

group members will modernize their location and estimation will be done again from the food to the source. Local leader renews its most excellent location inside the group, when the food source is not rationalized, then the group will start probing in different directions for the food sources. Two most important control parameters are GLlimit and LLlimit which give appropriate way to global and local leaders correspondingly. Levy flight has been intermingled in the algorithm to enhance the search ability. Proposed AMOA accelerates the exploitation ability. Proposed algorithm has been tested in standard IEEE 14, 30, 57,118,300 bus test system and simulation results show the projected algorithm reduced the real power loss extensively.

2. Problem Formulation

Objective of the problem is to reduce the true power loss:

$$F = P_L = \sum_{k\in Nbr}\ g_k\left(V_i^2 + V_j^2 - 2V_iV_j\cos\theta_{ij}\right). \quad \textbf{(1)}$$

Voltage deviation given as follows:

$$F = P_L + \omega_v \times \text{Voltage Deviation}. \quad \textbf{(2)}$$

Voltage deviation given by:

$$\text{Voltage Deviation} = \sum_{i=1}^{Npq}|V_i - 1|, \quad \textbf{(3)}$$

Constraint (equality):

$$P_G = P_D + P_L, \quad \textbf{(4)}$$

Constraints (inequality):

$$P_{gslack}^{min} \le P_{gslack} \le P_{gslack}^{max}, \quad \textbf{(5)}$$

$$Q_{gi}^{min} \le Q_{gi} \le Q_{gi}^{max}, i \in N_g, \quad \textbf{(6)}$$

$$V_i^{min} \le V_i \le V_i^{max}, i \in N, \quad \textbf{(7)}$$

$$T_i^{min} \le T_i \le T_i^{max}, i \in N_T, \quad \textbf{(8)}$$

$$Q_c^{min} \le Q_c \le Q_C^{max}, i \in N_C. \quad \textbf{(9)}$$

3. Augmented Monkey Optimization Algorithm

Communal behavior of monkeys has been utilized to model the algorithm. Normally, group monkeys assess the distance from the source to food for foraging behavior. Based on the distance from the foods source, the group members will modernize their location and estimation will be done again from the food to the source. Local leader renews its most excellent location inside the group, when the food source is not rationalized then the group will start probing in different

directions for the food sources [17]. Two most important control parameters are GLlimit and LLlimit which give appropriate way to global and local leaders correspondingly.

Population Initialization. Primary population of "N" monkeys where each monkey SM_i (i = 1, 2, ..., N) is a vector of dimension D. Every monkey (SM_i) is initialized by:

$$SM_{ij} = SM_{min\,j} + \emptyset \times \left(SM_{max\,j} - SM_{min\,j}\right). \quad \textbf{(10)}$$

Local Leader Phase (LLP). For new-fangled location, the fitness value will be computed. Updating of locations will be done based on the fitness value.

$$SM_{newij} = SM_{ij} + \emptyset_1 \times \left(LL_{kj} - SM_{ij}\right) + \emptyset_2 \times \left(SM_{rj} - SM_{ij}\right), \quad \textbf{(11)}$$

where $\emptyset_1 \in (0,1)$and $\emptyset_2 \in (-1,1)$.

Global Leader Phase (GLP). In this phase all the SMs modernize their location by Global Leader and local group member's indulgent and done by:

$$SM_{newij} = SM_{ij} + \emptyset_1 \times \left(GL_j - SM_{ij}\right) + \emptyset_2 \times \left(SM_{rj} - SM_{ij}\right), \quad \textbf{(12)}$$

where $\emptyset_1 \in (0,1)$and $\emptyset_2 \in (-1,1)$.

In GLP phase, monkey's (SM_i) locations are rationalized based on probability pi and computed by:

$$p_i = 0.90 \times \frac{fitness_i}{fitness_{maximum}} + 0.10. \quad \textbf{(13)}$$

Global Leader Learning (GLL) Phase. Global leader location is rationalized by applying the voracious selection procedure in the population, the stupendous fitness in the population is chosen as the rationalized location of the global leader. Additionally, when global leader is not updated then global limit count is incremented by 1.

Local Leader Learning (LLL) Phase. Local leader position is rationalized by employing the greedy selection, the rationalized location of the local leader is evaluated by comparing with the older one; when the local leader is not rationalized then the local limit count is incremented by 1.

Local Leader Decision (LLD) Phase. All members of group renew their locations by capricious initialization when the local leader position is not modernized,

$$SM_{newij} = SM_{ij} + \emptyset \times \left(GL_j - SM_{ij}\right) + \emptyset \times \left(SM_{ij} - LL_{kj}\right), \quad \textbf{(14)}$$

where $\emptyset \in (0,1)$.

Global Leader Decision (GLD) Phase. Global leader split the population into smaller groups when the position of global leader is not modernized and at first population is alienated into two groups, then three groups and so on until maximum number of groups are formed. Every time in GLD segment, LLL process is instigate to make a decision on the local leader in the newly formed groups.

Levy flight is a rank of non-Gaussian random procedure whose capricious walks are haggard from levy stable distribution. Allocation by $L(s) \sim |s|^{-1-\beta}$ where $0 < ß < 2$ is an index, scientifically defined as:

$$L(s,\gamma,\mu) = \begin{cases} \sqrt{\frac{\gamma}{2\pi}} & \exp\left[-\frac{\gamma}{2(s-\mu)}\right]\frac{1}{(s-\mu)^{3/2}} \quad \text{if } 0 < \mu < s < \infty. \\ 0 \quad \text{if } s \le 0 \end{cases} \tag{15}$$

In terms of Fourier transform, the levy distribution defined as:

$$F(k) = \exp\left[-\alpha|k|^{\beta}\right], 0 < \beta \le 2, \tag{16}$$

fresh state is calculated as:

$$X^{t+1} = X^{t} + \alpha \oplus \text{Levy } (\beta), \tag{17}$$

$$X^{t+1} = X^{t} + \text{random}\left(\text{size}(D)\right) \oplus \text{Levy}(\beta), \tag{18}$$

non-trivial scheme of engendering step size is defined by:

$$X^{t+1} = X^{t} + \text{random}\left(\text{size}(D)\right) \oplus \text{Levy}(\beta) \sim 0.01\frac{u}{|v|^{1/\beta}}\left(x_j^t - gb\right), \tag{19}$$

$$u \sim N(0,\sigma_u^2) \quad v \sim N(0,\sigma_v^2), \tag{20}$$

with

$$\sigma_u = \left\{\frac{\Gamma(1+\beta)\sin(\pi\beta/2)}{\Gamma[(1+\beta)/2]\beta 2^{(\beta-1)/2}}\right\}^{1/\beta}, \sigma_v = 1. \tag{21}$$

Here Γ is standard Gamma function. One of the important points to be considered while performing distribution by levy flights is the value taken by the β parameter and it substantially affects distribution.

To accelerate the exploitation ability of the monkey algorithm, a Levy Flight Based Local Search (LFLS) scheme is integrated with it.

In LFLS scheme step size is computed as:

$$\text{Step\_size} = 0.002 \times s(t) \times \left(x_{bestj} - x_{kj}\right) \times U(0,1), \tag{22}$$

position renewal of the most excellent individual inside the present population is found by:

$$x'_{bestj}(t+1) = x_{bestj}(t) + Step\_size(t). \quad \textbf{(23)}$$

Key in the optimization function Min f(x) and β;
Choose the most excellent solution x_{best},
Initialize t = 1, $\sigma_v = 1$,
Compute $\sigma_u = \left\{\frac{\Gamma(1+\beta)\sin(\pi\beta/2)}{\Gamma[(1+\beta)/2]\beta 2^{(\beta-1)/2}}\right\}^{1/\beta}$,
While $(t < \in)$ do,
Calculate the step size by; $Step_{size} = 0.002 \times s(t) \times (x_{bestj} - x_{kj}) \times U(0,1)$,
Engender a new-fangled solution x'_{best},
Compute $f(x'_{best})$; when $f(x'_{best}) = f(x_{best})$ then $x_{best} = x'_{best}$,
End if,
t = t + 1;
End while.

Levy flight has been intermingled in the algorithm to enhance the search ability. Proposed AMOA accelerates the exploitation ability.

Parameters values are initialized;
While stop criteria do;
Step a. Apply Local Leader phase.
Step b. Apply Global Leader phase.
Step c. Apply Local Leader Learning phase.
Step d. Apply Global Leader Learning phase.
Step e. Apply Local Leader Decision phase.
Step f. Apply Global Leader Decision phase.
Step g. Apply Levy Flight based Local Search Strategy
End while.
Print the most excellent solution.

4. Simulation Results

At first, in standard IEEE 14 bus system, the validity of the proposed AMOA has been tested, ***Table 1*** shows the constraints of control variables ***Table 2*** shows the limits of reactive power generators and comparison results are presented in ***Table 3***.

Table 1. Constraints of control variables.

System	Variables	Minimum (PU)	Maximum (PU)
	Generator Voltage	0.95	1.1
	Transformer Tap	o.9	1.1
	VAR Source	0	0.20

Table 2. Constrains of reactive power generators.

System	Variables	Q Minimum (PU)	Q Maximum (PU)
	1	0	10
	2	-40	50
	3	0	40
	6	-6	24
	8	-6	24

Table 3. Simulation results of IEEE −14 system.

Control variables	Base case	MPSO [19]	PSO [19]	EP [19]	SARGA [19]	AMOA
$VG-1$	1.060	1.100	1.100	NR*	NR*	1.010
$VG-2$	1.045	1.085	1.086	1.029	1.060	1.031
$VG-3$	1.010	1.055	1.056	1.016	1.036	1.022
$VG-6$	1.070	1.069	1.067	1.097	1.099	1.030
$VG-8$	1.090	1.074	1.060	1.053	1.078	1.014
Tap 8	0.978	1.018	1.019	1.04	0.95	0.902
Tap 9	0.969	0.975	0.988	0.94	0.95	0.910
Tap 10	0.932	1.024	1.008	1.03	0.96	0.950
$QC-9$	0.19	14.64	0.185	0.18	0.06	0.161
PG	272.39	271.32	271.32	NR*	NR*	272.06
QG (Mvar)	82.44	75.79	76.79	NR*	NR*	75.02
Reduction in PLoss (%)	0	9.2	9.1	1.5	2.5	16.9
Total PLoss (Mw)	13.550	12.293	12.315	13.346	13.216	11.256

NR* - Not reported.

Then the proposed AMOA has been tested in IEEE 30 bus system. ***Table 4*** shows the constraints of control variables, ***Table 5*** shows the limits of reactive power generators, and comparison results are presented in ***Table 6***.

Table 4. Constraints of control variables.

System	Variables	Minimum (PU)	Maximum (PU)
	Generator Voltage	0.95	1.1
	Transformer Tap	o.9	1.1
	VAR Source	0	0.20

Table 5. Constrains of reactive power generators.

System	Variables	Q Minimum (PU)	Q Maximum (PU)
	1	0	10
	2	-40	50
	5	-40	40
	8	-10	40
	11	-6	24
	13	-6	24

Table 6. Simulation results of IEEE −30 system.

Control variables	Base case	MPSO [19]	PSO [19]	EP [19]	SARGA [19]	AMOA
VG−1	1.060	1.101	1.100	NR*	NR*	1.023
VG−2	1.045	1.086	1.072	1.097	1.094	1.046
VG−5	1.010	1.047	1.038	1.049	1.053	1.078
VG−8	1.010	1.057	1.048	1.033	1.059	1.015
VG−12	1.082	1.048	1.058	1.092	1.099	1.059
VG-13	1.071	1.068	1.080	1.091	1.099	1.061
Tap11	0.978	0.983	0.987	1.01	0.99	0.901
Tap12	0.969	1.023	1.015	1.03	1.03	0.932
Tap15	0.932	1.020	1.020	1.07	0.98	0.901
Tap36	0.968	0.988	1.012	0.99	0.96	0.910
QC10	0.19	0.077	0.077	0.19	0.19	0.082
QC24	0.043	0.119	0.128	0.04	0.04	0.139
PG (MW)	300.9	299.54	299.54	NR*	NR*	299.01
QG (Mvar)	133.9	130.83	130.94	NR*	NR*	131.06
Reduction in PLoss (%)	0	8.4	7.4	6.6	8.3	10.6
Total PLoss (Mw)	17.55	16.07	16.25	16.38	16.09	15.68

NR* - Not reported.

Then the proposed AMOA has been tested in IEEE 57 bus system. ***Table 7*** shows the constraints of control variables, ***Table 8*** shows the limits of reactive power generators, and comparison results are presented in ***Table 9***.

Table 7. Constraints of control variables.

System	Variables	Minimum (PU)	Maximum (PU)
	Generator Voltage	0.95	1.1
	Transformer Tap	0.9	1.1
	VAR Source	0	0.20

Table 8. Constrains of reactive power generators.

System	Variables	Q Minimum (PU)	Q Maximum (PU)
	1	-140	200
	2	-17	50
	3	-10	60
	6	-8	25
	8	-140	200
	9	-3	9
	12	-150	155

Table 9. Simulation results of IEEE −57 system.

Control variables	Base case	MPSO [19]	PSO [19]	CGA [19]	AGA [19]	AMOA
VG 1	1.040	1.093	1.083	0.968	1.027	1.010
VG 2	1.010	1.086	1.071	1.049	1.011	1.021
VG 3	0.985	1.056	1.055	1.056	1.033	1.043
VG 6	0.980	1.038	1.036	0.987	1.001	1.021
VG 8	1.005	1.066	1.059	1.022	1.051	1.043
VG 9	0.980	1.054	1.048	0.991	1.051	1.001
VG 12	1.015	1.054	1.046	1.004	1.057	1.063
Tap 19	0.970	0.975	0.987	0.920	1.030	0.961`
Tap 20	0.978	0.982	0.983	0.920	1.020	0.940
Tap 31	1.043	0.975	0.981	0.970	1.060	0.932
Tap 35	1.000	1.025	1.003	NR*	NR*	1.010
Tap 36	1.000	1.002	0.985	NR*	NR*	1.001
Tap 37	1.043	1.007	1.009	0.900	0.990	1.000
Tap 41	0.967	0.994	1.007	0.910	1.100	0.991
Tap 46	0.975	1.013	1.018	1.100	0.980	1.014
Tap 54	0.955	0.988	0.986	0.940	1.010	0.982
Tap 58	0.955	0.979	0.992	0.950	1.080	0.961
Tap 59	0.900	0.983	0.990	1.030	0.940	0.973
Tap 65	0.930	1.015	0.997	1.090	0.950	1.012
Tap 66	0.895	0.975	0.984	0.900	1.050	0.976
Tap 71	0.958	1.020	0.990	0.900	0.950	1.013
Tap 73	0.958	1.001	0.988	1.000	1.010	1.001
Tap 76	0.980	0.979	0.980	0.960	0.940	0.972
Tap 80	0.940	1.002	1.017	1.000	1.000	1.001
QC 18	0.1	0.179	0.131	0.084	0.016	0.170
QC 25	0.059	0.176	0.144	0.008	0.015	0.172
QC 53	0.063	0.141	0.162	0.053	0.038	0.141
PG (MW)	1278.6	1274.4	1274.8	1276	1275	1261.4
QG (Mvar)	321.08	272.27	276.58	309.1	304.4	270.84
Reduction in PLoss (%)	0	15.4	14.1	9.2	11.6	18.5
Total PLoss (Mw)	27.8	23.51	23.86	25.24	24.56	22.642

NR* - Not reported.

Then the proposed AMOA has been tested in IEEE 118 bus system. ***Table 10*** shows the constraints of control variables and comparison results are presented in ***Table 11***.

Table 10. Constraints of control variables.

System	Variables	Minimum (PU)	Maximum (PU)
	Generator Voltage	0.95	1.1
	Transformer Tap	0.9	1.1
	VAR Source	0	0.20

Table 11. Simulation results of IEEE −118 system.

Control variables	Base case	MPSO [19]	PSO [19]	PSO [19]	CLPSO [19]	AMOA
VG 1	0.955	1.021	1.019	1.085	1.033	1.024
VG 4	0.998	1.044	1.038	1.042	1.055	1.040
VG 6	0.990	1.044	1.044	1.080	0.975	1.020
VG 8	1.015	1.063	1.039	0.968	0.966	1.013
VG 10	1.050	1.084	1.040	1.075	0.981	1.027
VG 12	0.990	1.032	1.029	1.022	1.009	1.018
VG 15	0.970	1.024	1.020	1.078	0.978	1.014
VG 18	0.973	1.042	1.016	1.049	1.079	1.039
VG 19	0.962	1.031	1.015	1.077	1.080	1.015
VG 24	0.992	1.058	1.033	1.082	1.028	1.028
VG 25	1.050	1.064	1.059	0.956	1.030	1.048
VG 26	1.015	1.033	1.049	1.080	0.987	1.036
VG 27	0.968	1.020	1.021	1.087	1.015	0.925
VG31	0.967	1.023	1.012	0.960	0.961	0.949
VG 32	0.963	1.023	1.018	1.100	0.985	0.961
VG 34	0.984	1.034	1.023	0.961	1.015	1.024
VG 36	0.980	1.035	1.014	1.036	1.084	1.018
VG 40	0.970	1.016	1.015	1.091	0.983	0.979
VG 42	0.985	1.019	1.015	0.970	1.051	1.019
VG 46	1.005	1.010	1.017	1.039	0.975	1.016
VG 49	1.025	1.045	1.030	1.083	0.983	1.004
VG 54	0.955	1.029	1.020	0.976	0.963	0.954
VG 55	0.952	1.031	1.017	1.010	0.971	0.982
VG56	0.954	1.029	1.018	0.953	1.025	0.969
VG 59	0.985	1.052	1.042	0.967	1.000	0.984
VG 61	0.995	1.042	1.029	1.093	1.077	0.982
VG 62	0.998	1.029	1.029	1.097	1.048	0.990
VG 65	1.005	1.054	1.042	1.089	0.968	1.001
VG 66	1.050	1.056	1.054	1.086	0.964	1.001
VG 69	1.035	1.072	1.058	0.966	0.957	1.051
VG 70	0.984	1.040	1.031	1.078	0.976	1.047
VG 72	0.980	1.039	1.039	0.950	1.024	1.039
VG 73	0.991	1.028	1.015	0.972	0.965	1.020
VG 74	0.958	1.032	1.029	0.971	1.073	1.029
VG 76	0.943	1.005	1.021	0.960	1.030	1.012
VG 77	1.006	1.038	1.026	1.078	1.027	1.032
VG 80	1.040	1.049	1.038	1.078	0.985	1.016
VG 85	0.985	1.024	1.024	0.956	0.983	1.025
VG 87	1.015	1.019	1.022	0.964	1.088	1.019
VG 89	1.000	1.074	1.061	0.974	0.989	1.053
VG 90	1.005	1.045	1.032	1.024	0.990	1.041

Control variables	Base case	MPSO [19]	PSO [19]	PSO [19]	CLPSO [19]	AMOA
VG 91	0.980	1.052	1.033	0.961	1.028	1.038
VG 92	0.990	1.058	1.038	0.956	0.976	1.029
VG 99	1.010	1.023	1.037	0.954	1.088	1.008
VG 100	1.017	1.049	1.037	0.958	0.961	1.014
VG 103	1.010	1.045	1.031	1.016	0.961	1.025
VG 104	0.971	1.035	1.031	1.099	1.012	1.014
VG 105	0.965	1.043	1.029	0.969	1.068	1.061
VG 107	0.952	1.023	1.008	0.965	0.976	1.020
VG 110	0.973	1.032	1.028	1.087	1.041	1.016
VG 111	0.980	1.035	1.039	1.037	0.979	1.014
VG 112	0.975	1.018	1.019	1.092	0.976	1.090
VG 113	0.993	1.043	1.027	1.075	0.972	1.028
VG 116	1.005	1.011	1.031	0.959	1.033	1.000
Tap 8	0.985	0.999	0.994	1.011	1.004	0.949
Tap 32	0.960	1.017	1.013	1.090	1.060	1.003
Tap 36	0.960	0.994	0.997	1.003	1.000	0.951
Tap 51	0.935	0.998	1.000	1.000	1.000	0.942
Tap 93	0.960	1.000	0.997	1.008	0.992	1.000
Tap 95	0.985	0.995	1.020	1.032	1.007	0.989
Tap 102	0.935	1.024	1.004	0.944	1.061	1.014
Tap 107	0.935	0.989	1.008	0.906	0.930	0.965
Tap 127	0.935	1.010	1.009	0.967	0.957	1.002
QC 34	0.140	0.049	0.048	0.093	0.117	0.014
QC 44	0.100	0.026	0.026	0.093	0.098	0.010
QC 45	0.100	0.196	0.197	0.086	0.094	0.172
QC 46	0.100	0.117	0.118	0.089	0.026	0.114
QC 48	0.150	0.056	0.056	0.118	0.028	0.031
QC 74	0.120	0.120	0.120	0.046	0.005	0.128
QC 79	0.200	0.139	0.140	0.105	0. 148	0.119
QC 82	0.200	0.180	0.180	0.164	0.194	0.165
QC 83	0.100	0.166	0.166	0.096	0.069	0.148
QC 105	0.200	0.189	0.190	0.089	0.090	0.161
QC 107	0.060	0.128	0.129	0.050	0.049	0.128
QC 110	0.060	0.014	0.014	0.055	0.022	0.014
PG(MW)	4374.8	4359.3	4361.4	NR*	NR*	4422.5
QG(MVAR)	795.6	604.3	653.5	* NR*	NR*	627.9
Reduction in PLOSS(%)	0	11.7	10.1	0.6	1.3	13.3
Total PLOSS (Mw)	132.8	117.19	119.34	131.99	130.96	115.01

NR* - Not reported.

Then IEEE 300 bus system [18] is used as test system to validate the performance of the AMOA. ***Table 12*** shows the comparison of real power loss obtained after optimization. ***Figure 1*** shows IEEE 300 bus system [18] and this IEEE 300-bus system contains 69 generators, 60 LTCs, 304 transmission lines, and 195 loads.

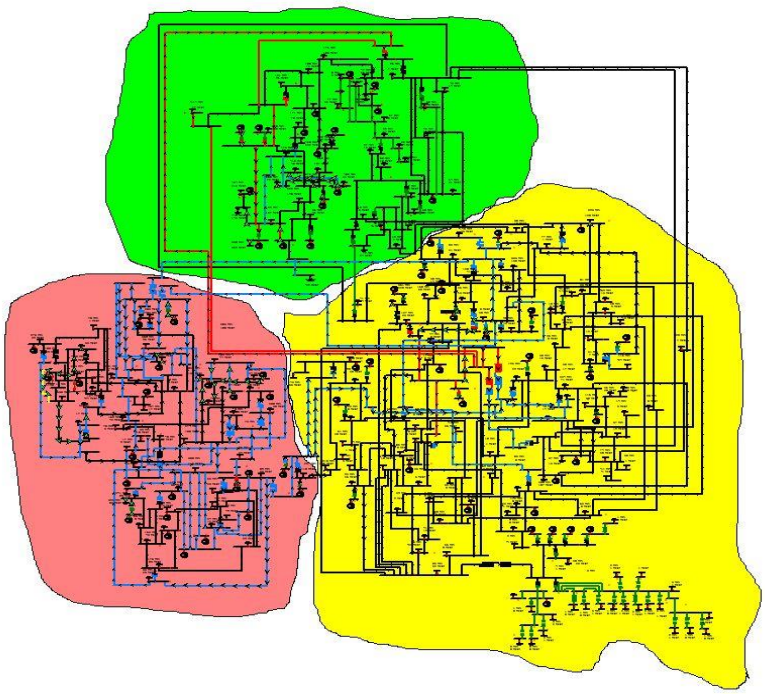

Figure 1. IEEE 300-Bus System case [18].

Table 12. Comparison of real power loss.

Parameter	Method EGA [21]	Method EEA [21]	Method CSA [20]	AMOA
PLOSS (MW)	646.2998	650.6027	635.8942	610.0964

5. Conclusion

In this work AMOA successfully solved the optimal reactive power problem. Two most important control parameters are GLlimit and LLlimit which give appropriate way to global and local leaders correspondingly. Levy flight has been intermingled in the algorithm to enhance the search ability. Proposed AMOA accelerated the exploitation ability. Proposed has been tested in standard IEEE 14, 30, 57,118,300 bus test systems and simulation results show the projected algorithm reduced the real power loss comprehensively.

References

[1] Lee, K. Y., Park, Y. M., & Ortiz, J. L. (1984, May). Fuel-cost minimisation for both real-and reactive-power dispatches. In *IEE proceedings C (generation, transmission and distribution)*, *131*(3), 85-93.

[2] Deeb, N. I., & Shahidehpour, S. M. (1988). An efficient technique for reactive power dispatch using a revised linear programming approach. *Electric power systems research*, *15*(2), 121-134.

[3] Bjelogrlic, M., Calovic, M. S., Ristanovic, P., & Babic, B. S. (1990). Application of newton's optimal power flow in voltage/reactive power control. *IEEE transactions on power systems*, *5*(4), 1447-1454.

[4] Granville, S. (1994). Optimal reactive dispatch through interior point methods. *IEEE transactions on power systems*, *9*(1), 136-146.

[5] Grudinin, N. (1998). Reactive power optimization using successive quadratic programming method. *IEEE Transactions on power systems*, *13*(4), 1219-1225.

[6] Mahate, R. K., & Singh, H. (2019). Multi-objective optimal reactive power dispatch using differential evolution. *International journal of engineering technologies and management research*, *6*(2), 27-38.

[7] Yalçın, E., Taplamacıoğlu, M. C., & Çam, E. (2019). The adaptive chaotic symbiotic organisms search algorithm proposal for optimal reactive power dispatch problem in power systems. *Electrica*, *19*(1), 37-47.

[8] Naderi, E., Narimani, H., Fathi, M., & Narimani, M. R. (2017). A novel fuzzy adaptive configuration of particle swarm optimization to solve large-scale optimal reactive power dispatch. *Applied soft computing*, *53*, 441-456.

[9] Heidari, A. A., Abbaspour, R. A., & Jordehi, A. R. (2017). Gaussian bare-bones water cycle algorithm for optimal reactive power dispatch in electrical power systems. *Applied soft computing*, *57*, 657-671.

[10] Morgan, M., Abdullah, N. R. H., Sulaiman, M. H., Mustafa, M., & Samad, R. (2016). Benchmark studies on optimal reactive power dispatch (ORPD) based multi-objective evolutionary programming (MOEP) using mutation based on adaptive mutation operator (AMO) and polynomial mutation operator (PMO). *Journal of electrical systems*, *12*(1), 121-132.

[11] Mouassa, S., Bouktir, T., & Salhi, A. (2017). Ant lion optimizer for solving optimal reactive power dispatch problem in power systems. *Engineering science and technology, an international journal*, *20*(3), 885-895.

[12] Anbarasan, P., & Jayabarathi, T. (2017, April). Optimal reactive power dispatch problem solved by symbiotic organism search algorithm. *2017 innovations in power and advanced computing technologies (i-PACT)* (pp. 1-8). Vellore, India: IEEE.

[13] Tighzert, L., Fonlupt, C., & Mendil, B. (2019). Towards compact swarm intelligence: a new compact firefly optimisation technique. *International journal of computer applications in technology*, *60*(2), 108-123.

[14] Gosain, A., & Sachdeva, K. (2019). Selection of materialized views using stochastic ranking based Backtracking Search Optimization Algorithm. *International journal of system assurance engineering and management*, *10*(4), 801-810.

[15] Basu, M. (2016). Quasi-oppositional differential evolution for optimal reactive power dispatch. *International journal of electrical power & energy systems*, *78*, 29-40.

[16] Weise, T. (2009). *Global optimization algorithms-theory and application*. Thomas Weise.

[17] Bansal, J. C., Sharma, H., Jadon, H. S., & Clerc, M. Spider Monkey optimization algorithm for numerical optimization. *Memetic Computing*, *6*, 31–47.

[18] IEEE 300 bus test. (1993). Retrieved October 01, 2019, from http://www.fglongatt.org/Test_Systems/IEEE_300bus.html

[19] Hussain, A. N., Abdullah, A. A., & Neda, O. M. (2018). Modified particle swarm optimization for solution of reactive power dispatch. *Research journal of applied sciences, engineering and technology*, *15*(8), 316-327.

[20] Reddy, S. S. (2017). Optimal reactive power scheduling using cuckoo search algorithm. *International journal of electrical & computer engineering*, *7*(5).

[21] Reddy, S. S., Bijwe, P. R., & Abhyankar, A. R. (2014). Faster evolutionary algorithm based optimal power flow using incremental variables. *International journal of electrical power & energy systems*, *54*, 198-210.